JOC Featured Article

# Dineopentyl Phosphate Hydrolysis: Evidence for Stepwise Water Attack

Shina C. L. Kamerlin,*,† Nicholas H. Williams,*,‡ and Arieh Warshel*,†

*Department of Chemistry, SGM 418, University of Southern California, 3620 McClintock Avenue, Los Angeles, California 90089, and Centre for Biological Chemistry, Department of Chemistry, University of Sheffield, Sheffield S3 7HF, U.K.*

*l.kamerlin@gmx.at; warshel@usc.edu; n.h.williams@sheffield.ac.uk*

*Received June 4, 2008*

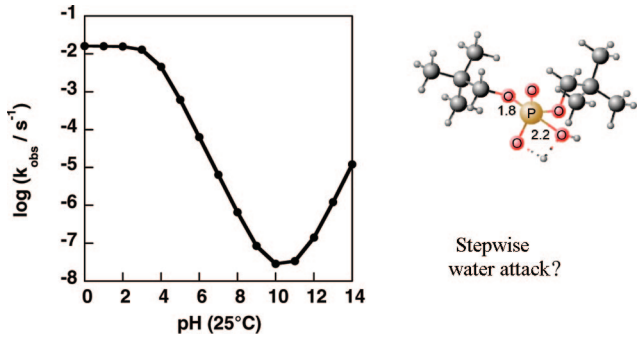


Phosphate ester hydrolysis is ubiquitous in biology, playing a central role in energy production, signaling, biosynthesis, and the regulation of protein function among other things. Although the mechanism of action of the enzymes regulating this reaction has been the focus of intensive research in the past few decades, the correct description of this apparently simple reaction remains controversial. A clear understanding of the mechanism that takes place in solution is crucial to be able to evaluate whether proposals for the enzyme-catalyzed mechanisms are reasonable. For the pH-independent hydrolysis of phosphate diesters, several kinetically equivalent mechanisms are plausible, including hydroxide attack on the neutral phosphate. However, it is very difficult to measure the rate of this reaction directly by experimental methods, so it has been evaluated by examining the rate of hydrolysis of neutral phosphate triesters, where a methyl group has replaced a proton. This may not be an accurate model of the neutral phosphate diester and does not provide information about a reaction pathway that is concerted with nucleophilic attack to generate a similar phosphorane. We have carefully mapped out free energy surfaces for both hydroxide and water attack on the dineopentyl phosphate anion and for water attack on the neutral diester. In doing so, we have accurately reproduced existing experimental data and demonstrate that water attack proceeds through an associative mechanism with proton transfer to the phosphate to generate a phosphorane intermediate. Our data show that the substrate-as-base mechanism is viable for phosphate ester hydrolysis, which may have important implications for the studies of phosphate ester hydrolysis by enzymes.

## Introduction

Phosphoryl transfer reactions are ubiquitous in biology, being involved in processes ranging from energy and signal transduction to the replication of genetic material.[1−7] In particular, phosphate diesters are used to hold together the genetic code in DNA and form the functional group that is manipulated by enzymes such as DNA polymerases, a family of enzymes that are responsible for regulating a wide range of activities including DNA recombination, repair, and damage bypassing, all of which are central to maintaining the integrity of the genome.[8] Thoroughly understanding the mechanism of phosphate diester hydrolysis in solution is central to further understanding the mechanism of diesterases such as DNA polymerases, the precise catalytic mechanism of which remains uncertain.[9−15]

* To whom correspondence should be addressed. Tel: 214-740-4114. Fax: 213-740-2701.
† University of Southern California.
‡ University of Sheffield.



10.1021/jo801207q CCC: $40.75 
Published on Web 08/27/2008

In contrast to phosphate monoesters, the uncatalyzed hydrolysis of phosphate diester monanions in solution is extremely slow.[16−18] For instance, the rate for the uncatalyzed hydrolysis of dimethyl phosphate at 25 °C is estimated to have a rate constant of approximately $2 \times 10^{-13}$ $s^{-1}$.[19] Additionally, the reaction has been found to proceed at least 99% by C−O cleavage, which is not the site of cleavage catalyzed by enzymes and which suggests an upper limit of approximately $1 \times 10^{-15}$ $s^{-1}$ (again at 25 °C) for the rate constant for spontaneous P−O cleavage.[20] This means that phosphodiesterases have to provide tremendous rate enhancements. For instance, staphylococcal nuclease accelerates the rate of P−O cleavage by at least $10^{16}$-fold,[21] or more specifically, computational studies obtain a difference of more than 35 kcal/mol if one compares the same reaction in solution and in the protein.[22,23] Computational studies have demonstrated that preorganized active sites with metal ions in the proper positions and with proper dielectric screening can account for the overall catalytic effect.[9,24] However, the detailed mechanism of the solution reaction remains controversial, and it is clearly vital to reach a consensus about this mechanism to be able to make progress in the elucidation of the precise mechanism in the active site of different phosphoryl transfer enzymes, particularly as different mechanisms have different requirements for catalysis.

The mechanism of phosphate monoester hydrolysis is a related problem of major biological interest.[2,20,25−28] In particular, it was considered that Ras catalyzed hydrolysis of GTP by using $Gln^{61}$ as a general base.[29−30] This is now generally disregarded, and it is accepted that the proton of the attacking water molecule ends up on the GTP being hydrolyzed[27,28,31−41] in a "substrate as base" mechanism,[28] though it is uncertain whether this proton is transferred in a stepwise or a concerted fashion.[33] Such a mechanism has been proposed for the hydrolysis of phosphate monoesters in solution,[42] though it has met with controversy.[37] This is based on comparing the

(1) Benkovic, S. J.; Schray, K. J. *Chemical Basis of Biological Phosphoryl Transfer*; Academic Press: New York, 1973; pp 201−238.
(2) Cleland, W. W.; Hengge, A. C. Enzymatic Mechanisms of Phosphate and Sulfate Transfer. *Chem. Rev.* **2006**, *106*, 3252–3278.
(3) Cor, J. R., Jr.; Ramsey, O. B. Mechanisms of Nucleophilic Substitution in Phosphate Esters. *Chem. Rev.* **1964**, *64*, 317–352.
(4) Kirby, J. A.; Warren, S. G. *The Organic Chemistry of Phosphorous*; Elsevier: Amsterdam, 1967.
(5) Mildvan, A. S. The Role of Metals in Enzyme-Catalyzed Substitutions at Each of the Phosphorous Atoms of ATP. *Adv. Enzymol. Relat. Areas Mol. Biol.* **1979**, *49*, 103–126.
(6) Vetter, I. R.; Wittinghofer, A. Nucleoside Triphosphate-Binding Proteins: Different Scaffolds to Achieve Phosphoryl Transfer. *Q. Rev. Biophys.* **1999**, *32*, 1–56.
(7) Westheimer, F. H. Monomeric Metaphosphates. *Chem. Rev.* **1981**, *64*, 317–352.
(8) Hübscher, U.; Maga, G.; Spadari, S. Eukaryotic DNA Polymerases. *Annu. Rev. Biochem.* **2002**, *71*, 133–163.
(9) Florián, J.; Goodman, M. F.; Warshel, A. Computer Simulations of the Chemical Catalysis of DNA Polymerases: Discriminating between Alternative Nucleotide Insertion Mechanisms for T7 DNA Polymerase. *J. Am. Chem. Soc.* **2003**, *125*, 8163–8177.
(10) Florián, J.; Goodman, M. F.; Warshel, A. Computer Simulations of Protein Functions: Searching for the Molecular Origin of the Replication Fidelity of DNA Polymerases. *Proc. Natl. Acad. Sci. U.S.A.* **2005**, *102*, 6819–6824.
(11) Xiang, Y.; Oelschlager, P.; Florián, J.; Goodman, M. F.; Warshel, A. Simulating the Effect of DNA Polymerase Mutations on Transition State Energetics and Fidelity: Evaluations Amino Acid Group Contributions and Allosteric Coupling for Ionized Residues in Human pol beta. *Biochemistry* **2006**, *45*, 7036–7048.
(12) Arndt, J. W.; Gong, W.; Xuejon, Z.; Showalter, A. K.; Liu, J.; Dunlap, C. A.; Lin, Z.; Paxson, C.; Tsai, M.-D.; Chan, M. K. Insight into the Catalytic Mechanism of DNA Polymerase beta: Structures of Intermediate Complexes. *Biochemistry* **2001**, *40*, 5368–5375.
(13) Wang, L.; Yu, X.; Hu, P.; Broyde, S.; Zhang, Y. A Water-Mediated and Substrate-Assisted Catalytic Mechanism for Sulfolobus Solfataricus and DNA Polymerase IV. *J. Am. Chem. Soc.* **2007**, *129*, 4731–4737.
(14) Petellier, H.; Sawaya, M. R.; Kumar, A.; Wilson, S. H.; Kraut, J. Structures of Ternary Complexes of Rat DNA Polymerase beta, a DNA Template-Primer and ddCTP. *Science* **1994**, *264*, 1893–1903.
(15) Lin, P.; Pedersen, L. C.; Batra, V. K.; Beard, W. A.; Wilson, S. H.; Pedersen, L. G. Energy Analysis of Chemistry for Correct Insertion by DNA Polymerase beta. *Proc. Natl. Acad. Sci. U.S.A.* **2006**, *103*, 13294–13299.
(16) Bunton, C. A.; Mhala, M. M.; Oldham, K. G.; vernon, C. A. The Reactions of Organic Phosphates. *J. Chem. Soc.* **1960**, *329*, 3–3301.
(17) Kumamoto, J.; Cox, J. R., Jr.; Westheimer, F. H. Barium Ethylene Phosphate. *J. Am. Chem. Soc.* **1956**, *78*, 4858–4860.
(18) Kirby, J. A.; Younas, M. The Reactivity of Phosphate Esters. *J. Chem. Soc. B.* **1970**, *51*, 0–513.
(19) Radzicka, A.; Wolfenden, R. A Proficient Enzyme. *Science* **1995**, *267*, 90–93.
(20) Wolfenden, R.; Ridgeway, C.; Young, G. Spontaneous Hydrolysis of Ionised Phosphate Monoesters and Diesters and the Proficiencies of the Phosphatases and Phosphodiesterases As Catalysts. *J. Am. Chem. Soc.* **1998**, *120*, 833–834.
(21) Mildvan, A. S. Mechanisms of Signaling and Related Enzymes. *Proteins: Structure, Function Genet.* **1997**, *29*, 401–416.
(22) Aqvist, J.; Warshel, A. Calculations of Free Energy Profiles for the Staphylococcal Nuclease Catalysed Reaction. *Biochemistry* **1989**, *28*, 4680–4689.
(23) Warshel, A.; Sharma, P. K.; Kato, M.; Xiang, Y.; Liu, H.; Olsson, M. H. Electrostatic Basis for Enzyme Catalysis. *Chem. Rev.* **2006**, *106*, 3210–3235.
(24) Fothergill, M.; Goodman, M. F.; Petruska, J.; Warshel, A. Structure energy analysis of the role of metal ions in phosphodiester bond hydrolysis by DNA Polymerase I. *J. Am. Chem. Soc.* **1995**, *117*, 11619–11627.
(25) Lad, C.; Williams, N. H.; Wolfenden, R. The Rate of Hydrolysis of Phosphomonoester Dianions and the Exceptional Catalytic Proficiencies of Protein and Inositol Phosphatases. *Proc. Natl. Acad. Sci. U.S.A.* **2003**, *100*, 5607–5610.
(26) Wolfenden, R. Degrees of Difficulty of Water-Consuming Reactions in the Absence of Enzymes. *Chem. Rev.* **2006**, *106*, 3379–3396.
(27) Klahn, M.; Rosta, E.; Warshel, A. On the Mechanism of Hydrolysis of Phosphate Monoester Dianions in Solution and Proteins. *J. Am. Chem. Soc.* **2006**, *128*, 15310–15323.
(28) Langen, R.; Schweins, T.; Warshel, A. On the Mechanism of Guanosine Triphosphate Hydrolysis in ras p21 Proteins. *Biochemistry* **1992**, *31*, 8691–8696.
(29) Pai, E. F.; Kabsch, W.; Krengel, U.; Holmes, K.; John, J.; Wittinghofer, A. Structure of the Guanine-Nucleotide Binding Domain of the Ha-ras Oncogene Produced p21 in the Triphosphate Conformation. *Nature* **1989**, *341*, 209–214.
(30) Pai, E. F.; Krengel, U.; Petsko, G. A.; Goody, R. S.; Kabsch, W.; Wittinghofer, A. Refined Crystal Structure of the Triphosphate Conformation of H-ras p21 at 1.35A Resolution: Implications for the Mechanism of GTP Hydrolysis. *EMBO J.* **1990**, *9*, 2351–2359.
(31) Schweins, T.; Langen, R.; Warshel, A. Why Have Mutagenesis Studies Not Located the General Base in ras p21. *Nat. Struct. Biol.* **1994**, *1*, 476–484.
(32) Schweins, T.; Geyer, M.; Scheffzek, K.; Warshel, A.; Kalbitzer, H. R.; Wittinghofer, A. Substrate-Assisted Catalysis As a Mechanism for GTP Hydrolysis of p21ras and Other GTP-Binding Proteins. *Nat. Struct. Biol.* **1995**, 36–44.
(33) Glennon, T. M.; Villa, J.; Warshel, A. How Does GAP Catalyse the GTPase Reaction of Ras? A Computer Simulation Study. *Biochemistry* **2000**, *39*, 9641–9651.
(34) Shurki, A.; Warshel, A. Why Does the Ras Switch "Break" by Oncogenic Mutations. *Proteins* **2004**, *55*, 1–10.
(35) Schweins, T.; Geyer, M.; Kalbitzer, H. R.; Wittinghofer, A.; Warshel, A. Linear Free Energy Relationships in the Intrinsic and Gtpase Activating Protein-Stimulated Guanosine 5′-Triphosphate Hydrolysis of p21ras. *Biochemistry* **1996**, *35*, 14225–14231.
(36) Admiraal, S. J.; Herschlag, D. Mapping the Transition State for ATP Hydrolysis: Implications for Enzymatic Catalysis. *Chem. Biol.* **1995**, *2*, 729–739.
(37) Admiraal, S. J.; Herschlag, D. The Substrate-Assisted General Base Catalysis Model for Phosphate Monoester Hydrolysis: Evaluation Using Reactivity Comparisons. *J. Am. Chem. Soc.* **2000**, *122*, 2145–2148.
(38) Maegley, K. A.; Admiraal, S. J.; Herschlag, D. Ras-Catalyzed Hydrolysis of GTP: A New Perspective from Model Studies. *Proc. Natl. Acad. Sci. U.S.A.* **1996**, *93*, 8160–8166.
(39) Schweins, T.; Warshel, A. Mechanistic Analysis of the Observed Linear Free Energy Relationships in p21ras and Related Systems. *Biochemistry* **1996**, *35*, 14232–14243.
(40) Grigorenko, B.; Nemukhin, A. V.; Cachau, R. E.; Topol, I. A.; Burt, S. K. Computational Study of a Transition State Analogue of Phosphoryl Transfer in the Ras-RasGAP Complex: AlFx versus MgF. *J. Phys. Chem. B.* **2006**, *11*, 503–508.
(41) Chung, H. H.; Benson, D. R.; Schultz, P. G. Probing the Structure and Mechanism of Ras Protein with an Expanded Genetic Code. *Science* **1993**, *5*, 806–809.
(42) Florian, J.; Warshel, A. A Fundamental Assumption about OH-Attack in Phosphate Hydrolysis Is Not Fully Justified. *J. Am. Chem. Soc.* **1997**, *119*, 4458–4472.

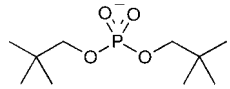

**FIGURE 1.** Dineopentyl phosphate ($NpO_2PO_2^-$).

rates for the hydrolysis of methyl phosphate[43] and trimethyl phosphate[43,44] and for the reactions of the monoanions of 2,4-dinitronitrophenyl phosphate and its diester analogue, methyl 2,4-dinitrophenyl phosphate, which suggest that the rate of reaction of the neutral species with hydroxide is too slow to compensate for the unfavorable equilibrium involved in transferring a proton from water to the phosphate. However, a computational study has suggested that the rate of hydroxide attack on neutral phosphate monoesters is much faster than for the corresponding triester,[42] suggesting that this mechanism should not be ruled out a priori. This paper considers whether these principles apply to phosphate diester hydrolysis.

Generally, phosphate ester hydrolysis can proceed via two limiting extremes: an associative pathway in which nucleophilic attack precedes phosphorus oxygen bond cleavage, and a dissociative pathway in which the leaving group departs prior to nucleophilic attack.[45,46] These limiting cases ($A_N + D_N$ or $D_N + A_N$) are in turn linked by a continuous spectrum of concerted ($A_ND_N$) pathways, where bond formation and cleavage occur simultaneously and there is a single transition state for the reaction. These are also associative reactions, but where the character of the transition state varies according to the degree of bonding to the nucleophile and leaving group. If there is a net increase in bonding, then it can be described as more associative in character; if there is a net decrease in bonding, it is more dissociative in character. While the interpretation of previous experimental studies with good leaving groups has suggested that phosphate diester hydrolysis proceeds through a single transition state,[47,48] the issue of whether the transition state is associative or dissociative in character is more difficult to address. Recent computational studies show that even for the homologous monoesters studied in ref.,[27] the transition state structure is sensitive to the nature of the leaving group. That is, while the mechanism is associative with higher p$K_a$ leaving groups, the transition states become progressively more dissociative in character as the p$K_a$ of the leaving group is decreased. Earlier studies have also demonstrated that the precise reaction path for phosphate ester hydrolysis is dependent on the p$K_a$ of the leaving group.[27,48]

Dineopentyl phosphate ($NpO_2PO_2^-$, Figure 1) is a useful model system for kinetic studies of the hydrolysis of phosphate diester with poor leaving groups through P−O cleavage, as C−O cleavage is selectively prevented by steric effects. At 250 °C,

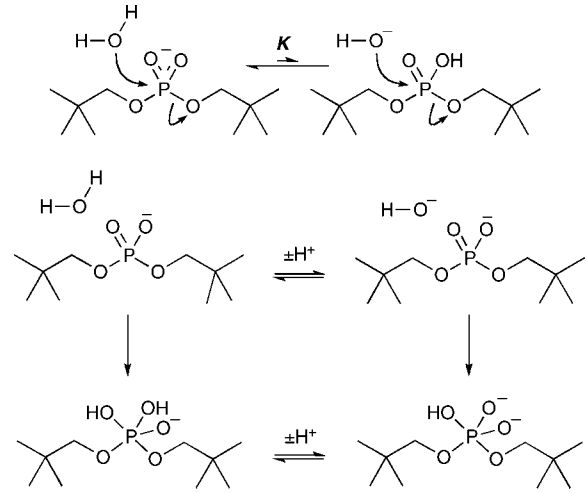

**FIGURE 2.** Alternative kinetically equivalent mechanisms for the pH-independent hydrolysis of the $NpO_2PO_2^-$ anion[49] and the ionization equilibria relating the pH-independent and hydroxide-promoted pathways.

the variation in the rate of hydrolysis with pH shows a wide pH-independent region, with base catalysis only becoming significant above pH 13. Most simply, this behavior can be accounted for by mechanisms where either water or hydroxide are the nucleophiles that attack the phosphate anion. However, it is possible that the diester is not hydrolyzed through water attack on the $NpO_2PO_2^-$ monoanion, but through the kinetically equivalent mechanism of hydroxide attack on neutral $NpO_2PO_2H$[49] (Figure 2). If this is the case, then both the high pH reaction and the pH-independent reaction could involve hydroxide attack at the phosphorus atom to form closely related phosphorane intermediates (or transition states; Figure 2). Interestingly, both regions have virtually identical activation parameters, which effectively means that this pH dependence will be similar under ambient conditions.[49] This observation might arise because a monoanionic phosphorane is believed[50] to have a p$K_a$ similar to that of water, so the loss of a proton from either will have a similar energy penalty and the equilibria in Figure 2 will be similar in magnitude, resulting in no net changes to the activation energies of the two reactions.

Experimentally, it is very difficult to make a clear distinction between these two mechanistic alternatives. Here, we address this issue by carefully mapping the free energy surface for $HO^-$ attack on neutral and anionic dineopentyl phosphate and $H_2O$ attack on the anion. The protocol used in this work is similar to that used in ref 27, where it was successfully applied to the study of phosphate monoesters.[27] It should be noted that the issue of water attack on dimethyl phosphate has already been examined in a recent computational study.[51] However, this work has not explicitly taken into account the possibility of water attack with proton migration by means of mapping the free energy surface using a More O'Ferrall−Jencks (MFJ) plot, thus making the conclusions problematic. More importantly, in contrast to this previous study, we have considered the reaction at all pHs and established a role for the proton migration. Here,

(43) Bunton, C. A.; Llewellyn, D. R.; Oldham, K. G.; Vernon, C. A. The Reactions of Organic Phosphates. *J. Chem. Soc.* **1958**, *77*, 3574–3587.

(44) Barnard, P. W. C.; Bunton, C. A.; Llewellyn, D. R.; Vernon, C. A.; Welch, C. A. The Reactions of Organic Phosphates. *J. Chem. Soc.* **1961**, *267*, 0–2676.

(45) Ba-Saif, S. A.; Davis, A. M.; Williams, A. J. Effective Charge Distrtibution for Attack of Phenoxide Ion on Aryl Methyl Phosphate Monoanion: Studies Related to the Action of Ribonuclease. *J. Org. Chem.* **1989**, *54*, 5483–5486.

(46) Barnes, J. A.; Wilkie, J.; Williams, I. H. Transition-State Structural Variation and Mechanistic Change. *J. Chem. Soc., Faraday Trans.* **1994**, *90*, 1709–1714.

(47) Zalatan, J. G.; Herschlag, D. Alkaline Phosphatases Mono- and Diesterase Reactions: Comparative Transition State Analysis. *J. Am. Chem. Soc.* **2006**, *128*, 1293–1303.

(48) Williams, N. H.; Cheung, J.; Chin, J. Reactivity of Phosphate Diesters Doubly Coordinated to a Dinuclear Cobalt(Iii) Complex: Dependence of the Reactivity on the Basicity of the Leaving Group. *J. Am. Chem. Soc.* **1998**, *120*, 8079–8087.

(49) Schroeder, G. K.; Lad, C.; Wyman, P.; Williams, N. H.; Wolfenden, R. The Time Required for Water Attack at the Phosphorus Atom of Simple Phosphodiesters and of DNA. *Proc. Natl. Acad. Sci. U.S.A.* **2006**, *103*, 4052–4055.

(50) Davies, J. E.; Doltsinis, N. L.; Kirby, A. J.; Roussev, C. D.; Sprik, M. Estimating p$K_a$ Values for Pentaoxyphosphoranes. *J. Am. Chem. Soc.* **2002**, *124*, 6594–6599.

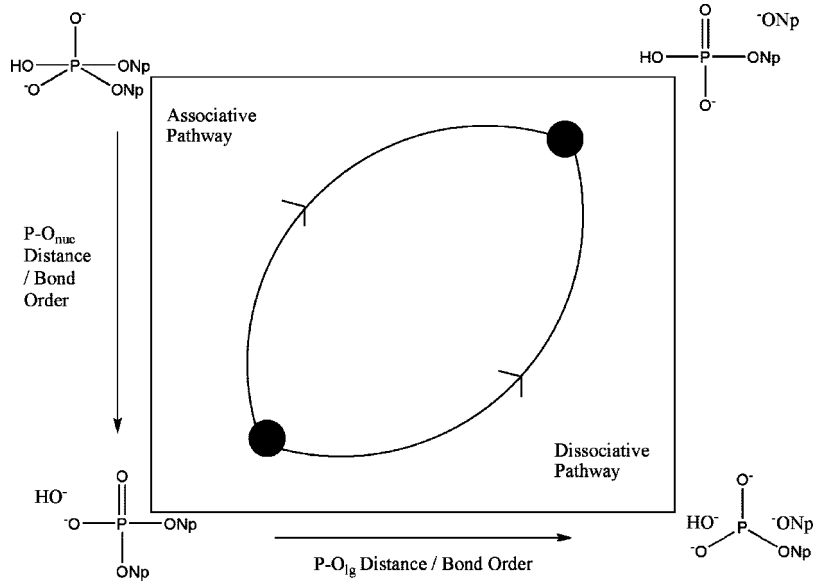


**FIGURE 3.** Defining potential reaction pathways on the free energy surface for hydroxide attack on the $NpO_2PO_2^-$ anion. The paths shown represent concerted ($A_ND_N$) mechanisms with different characters.

we demonstrate that while the base-catalyzed reaction (hydroxide attack on $NpO_2PO_2^-$) proceeds through a single-step mechanism ($A_ND_N$) with a compact (associative) transition state, the pH-independent reaction ($H_2O$ attack on $NpO_2PO_2^-$) proceeds through an associative ($A_N + D_N$) mechanism in which P−O bond formation is coupled with proton transfer from the attacking water molecule to a phosphate oxygen, yielding a pentavalent $A_N + D_N$ intermediate. If the reaction proceeds through a pre-equilibrium transfer of a proton from water to the phosphate, followed by an associative ($A_N + D_N$) mechanism, a similar overall activation energy results. Finally, both $A_ND_N$ and $A_N + D_N$ pathways are equally viable for the acid-catalyzed reaction ($H_2O$ attack on neutral $NpO_2PO_2H$).

**Theoretical Basis.** The most thorough computational approach toward studying the mechanism of phosphate ester hydrolysis in solution is by mapping out the full free energy surface for the system, a schematic example of which is shown in Figure 3. This is in effect a More O'Ferrall−Jencks diagram[52,53] in which the reaction surface is depicted in terms of bond lengths (rather than using bond orders or Leffler indices such as used, e.g., by Williams et al.;[45] overall, the two surfaces are similar in that they combine a two-dimensional measure of reaction progress with the energy of the system). Separate free energy surfaces were generated for hydroxide and water attack on dineopentyl phosphate. In each case, the reaction surface was defined in terms of two reaction coordinates: the phosphorus oxygen distances to the leaving group (R1, *x*-axis) and to the nucleophile (R2, *y*-axis), respectively. Each individual coordinate corresponds to multiple points in the full free energy description of the system as the other degrees of freedom in the system can vary. However, at each point, only the two degrees of freedom defining the reaction coordinate are constrained and all other degrees of freedom are allowed to freely optimize to define the surfaces shown. As any variation in an unconstrained degree of freedom not directly related to the reaction can cause unwanted noise on the free energy surface, obscuring the location of key stationary points, it is extremely important to generate the free energy surfaces using careful reaction coordinate pushing. Thus, the geometry and energy at each point was examined to ensure that the 2D plot obtained is the true lowest energy free energy surface.[27,54]

All ab initio calculations were performed using the Gaussian03 software package[55] and Becke's three-level hybrid functionals which combine Hartree−Fock exchange and density functional theory (DFT) exchange correlations.[56] At each point on the free energy surface, P−O distances to the leaving group and nucleophile oxygens were constrained, and all other degrees of freedom were allowed to optimize freely. These distances were mapped out in the range from 1.6 up to 3.4 Å, in 0.2 Å increments, except in the immediate vicinity of transition states where 0.1 Å increments were used for extra clarity. The 6-31+G* basis set was used to obtain initial gas-phase geometries, and solvation effects on the resulting structures were simulated by applying a solvation correction to the gas-phase geometries using the 6-311+G** basis set and the COSMO

(51) Iché-Tarrat, N.; Barthelat, J.-C.; Rinaldi, D.; Vigroux, A. Theoretical Studies of the Hydroxide-Catalyzed P−O Cleavage Reactions of Neutral Phosphate Triesters and Diesters in Aqeuous Solution: Examination of the Changes Induced by H/Me substitution. *J. Phys. Chem. B* **2005**, *109*, 22570–225800.

(52) Jencks, W. P. A Primer for the bema Hapothle. An Empirical Approach to the Characterization of Changing Transition-State Structures. *Chem. Rev.* **1985**, *85*, 511–527.

(53) More O'Ferrall, R. A. Relationships between E2 and E1cB Mechanisms of beta-Elimination. *J. Chem. Soc. B* **1970**, 274–277.

(54) Kamerlin, S. C. L.; Wilkie, J. The Role of Metal Ions in Phosphate Ester Hydrolysis. *Org. Biomol. Chem.* **2007**, *5*, 2098–2108.

(55) Frisch, M. J.; Trucks, G. W.; Schlegel, H. B.; Scuseria, G. E.; Robb, M. A.; Cheeseman, J. R.; Montgomery, J., J. A.; Vreven, T.; Kudin, K. N.; Burant, J. C.; Millam, J. M.; Iyengar, S. S.; Tomasi, J.; Barone, V.; Mennucci, B.; Cossi, M.; Scalmani, G.; Rega, N.; Petersson, G. A.; Nakatsuji, M.; Hada, M.; Ehara, K.; Toyota, R.; Fukuda, J.; Hasegawa, M.; Ishida, T.; Nakajima, Y.; Honda, Y.; Kitao, O.; Nakai, H.; Klene, M.; Li, X.; Knox, J. E.; Hratchian, H. P.; Cross, J. B.; Adacmo, C.; Jaramillo, J.; Gomperts, R.; Stratmann, R. E.; Yazyev, O.; Austin, A. J.; Cammi, R.; Pomelli, C.; Ochterski, J.; Ayala, P. Y.; Morokuma, K.; Voth, G. A.; Salvador, P.; Dannenberg, J. J.; Zakrzewski, V. G.; Dapprich, S.; Daniels, A. D.; Strain, M. C.; Farkas, O.; Malick, D. K.; Rabuck, A. D.; Clifford, K.; Cioslowki, J.; Stefanov, B. B.; Liu, G.; Liashenko, A.; Piskorz, P.; Komaromi, I.; Martin, R. L.; Fox, D. J.; Keith, T.; Al-Laham, M. A.; Peng, C. Y.; Nanayakkara, A.; Challacombe, M.; Gill, P. M. W.; Johnson, B. G.; Chen, W.; Wong, M. W.; Gonzalez, C.; Pople, J. A., *GAUSSIAN 03 (Revision C.02)*; Gaussian: Pittsburgh, PA, 2004.

(56) Becke, A. D., III. The Role of Exact Exchange. *J. Chem. Phys.* **1993**, *98*, 5648–5652.

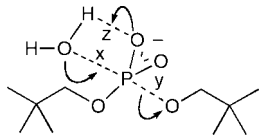

**FIGURE 4.** Potential reaction coordinates for a multidimensional free energy surface for water attack on dineopentyl phosphate with concomitant proton transfer to a phosphate oxygen.

continuum model.[57,58] The COSMO calculations were performed using the UFF model rather than the default UA0 model, to be able to account for any potential proton transfer between the attacking nucleophile and the phosphate. The free energy surfaces obtained were then used to identify the approximate location and energies of key stationary points relative to the sum of the energies of the diester and nucleophile at infinite separation.

An important issue when dealing with water attack on dineopentyl phosphate is the potential for proton transfer from the attacking water molecule onto a phosphate oxygen atom, as illustrated in Figure 2. This proton transfer would in effect introduce a third degree of freedom into the reaction, giving rise to a multidimensional reaction coordinate (Figure 4 shows the potential $x$, $y$, and $z$ coordinates for such a system).

It could be argued that such a system should be dealt with using a reaction cube[59] as proposed in ref 59, where the proton position would be included in the definition of the reaction coordinate. However, this is problematic on two accounts. First, even if the intramolecular general base mechanism is defined as a distinguishable path, this is not an independent pathway as the substrate is still the ultimate proton acceptor, and this property will change with the reaction progress. Furthermore, setting up the system as a three-dimensional cube is in effect forcing this proton transfer and so can obscure whether this is actually a desirable process. Therefore, we prefer to retain a two-dimensional free energy surface, where the proton of the attacking water is always allowed to find the lowest energy path at any point on the map. Thus, when proton transfer does occur, it has not been explicitly included in the definition of the associative versus dissociative pathway, similar to refs 27 and 54.

Finally, when studying phosphate ester hydrolysis, the overall activation entropy of the reaction needs to be taken into account. The activation entropy is composed of two terms: the solvent contribution ($-T\Delta S_{solv}$) and the solute contribution ($-T\Delta S_{conf}$). The former term (i.e., the solvation entropy) is implicitly evaluated by the solvation model (in this case COSMO), and while it is not possible to quantify the exact magnitude of the entropic contribution of this solvation model to the total free energy, it is considered that this contribution is not negligible.[60] However, the latter term (i.e., the configurational entropy) needs to be calculated explicitly. Traditionally, the correct calculation of configurational entropies has presented a significant computational challenge. We approach this problem by means of the restraint release approach,[61,62] which has been described in great detail in refs 61 and 62. The principle behind this approach is fairly straightforward and involves first imposing strong Cartesian constraints on the position of the solute atoms in both the reactant and transition states, and subsequently evaluating the free energy difference associated with the release of these restraints by use of a free energy perturbation approach (described in detail in ref 62), as shown in eq 1:

$$-T(\Delta S^{\ddagger})_{conf} = \min(\Delta G_{RR}^{TS}) - \min(\Delta G_{RR}^{RS}) + T\Delta S_{cage}^{RS} \quad (1)$$

An issue that cannot be neglected when utilizing the restraint release approach is the fact that all restraint release free energies include an enthalpic contribution.[62] Therefore, the entire procedure is repeated with different constraints in order to identify the restraint coordinates that minimize $G_{RR}$ in both transition and reactant states (denoted by $\min(\Delta G_{RR})$) in eq 1), which in turn minimizes the enthalpic contribution to $-T\Delta S_{conf}$. $\Delta S_{cage}$ is merely the entropy associated with applying a special ($K_{cage}$ = 0.3 kcal/mol/Å$^2$) restraint to a pair of reacting atoms in order to keep them at a specified contact distance, thus bringing the reactant fragment from a molar volume to the same solvent cage. This entropy term was rigorously and analytically evaluated as a function of a special restraint that was used to keep the fragment at a predefined contact distance as outlined in ref 62.

In order to save computational resources, it is expedient to replace eq 1 by

$$-TS_{conf} = -TS(K = K_1)_{QH} + \min(\Delta G_{RR}(K = K_1 \rightarrow K = 0)) \quad (2)$$

Here, $(K = K_1)_{QH}$ designates entropy computed by the quasiharmonic approximation,[63] where $\Delta G_{RR}$ once again denotes the restraint release free energy. Combining these two approaches takes advantage of the fact that the quasiharmonic approximation tends to be valid at significant restraints, and only becomes problematic upon the release of these restraints (as a range of very shallow anharmonic potential energy surfaces are reached). This combined approach has been successful in studies of the ribosome[61] as well as phosphate ester hydrolysis.[27] Since the FEP calculations cannot currently be performed with an ab initio surface, we have instead represented the reaction system by an EVB potential that approximates the ab initio surface. Our restraint release calculations were performed in both the reactant and transition states, where both molecules were placed in a 16 Å simulation sphere of explicit water molecules subjected to the SCAAS boundary conditions.[64] The RR-FEP calculations were done while changing $K_1$ from 10 kcal mol$^{-1}$ A$^{-2}$ to 0.0 kcal mol$^{-1}$ A$^{-2}$ in 41 mapping steps of 3 ps in length each using a 1 fs time step, at 300 K. The minimum value (i.e., $\min(\Delta G_{RR})$) was then taken from 10 series of runs. All

(57) Barone, V.; Cossi, M. Quantum Calculation of Molecular Energies and Energy Gradients in Solution by a Conductor Solvent Model. *J. Phys. Chem. A* **1998**, *102*, 1995–2001.

(58) Klamt, A.; Schüürmann, G. J. COSMO: a New Approach to Dielectric Screening in Solvents with Explicit Expressions for the Screening Energy and Its Gradient. *J. Chem. Soc., Perkin Trans. 2* **1993**, *5*, 799–805.

(59) Guthrie, J. P. Multidimensional Marcus Theory: An Analysis of Concerted Reactions. *J. Am. Chem. Soc.* **1996**, *118*, 12878–12885.

(60) Borden, J.; Crans, D. C.; Florián, J. Transition State Analogues for Nucleotidyl Transfer Reactions: Structure and Stability of Pentavalent Vanadate and Phosphate Ester Dianions. *J. Phys. Chem. B.* **2006**, *110*, 14988–14999.

(61) Sharma, P. K.; Xiang, Y.; Kato, M.; Warshel, A. What Are the Roles of Substrate Assisted Catalysis and Proximity Effects in Peptide Bond Formation by the Ribosome. *Biochemistry* **2005**, *44*, 11307–11314.

(62) Strajbl, M.; Sham, Y. Y.; Villa, J.; Chu, Z. T.; Warshel, A. Calculation of Activation Entropies of Chemical Reactions in Solution. *J. Phys. Chem. B.* **2000**, *104*, 4578–4584.

(63) Levy, R.; Karplus, M.; Kuschisk, J.; Perahia, D. Evaluation of the Configurational Entropy for Proteins - Application to Molecular Dynamics Simulations of an Alpha-Helix. *Macromolecules* **1984**, *17*, 1370–1374.

(64) Lee, F. S.; Chu, Z. T.; Warshel, A. Microscopic and Semimicroscopic Calculations of Electrostatic Energies in Proteins by the POLARIS and ENZYMIX Programs. *J. Comput. Chem.* **1993**, *14*, 161–185.

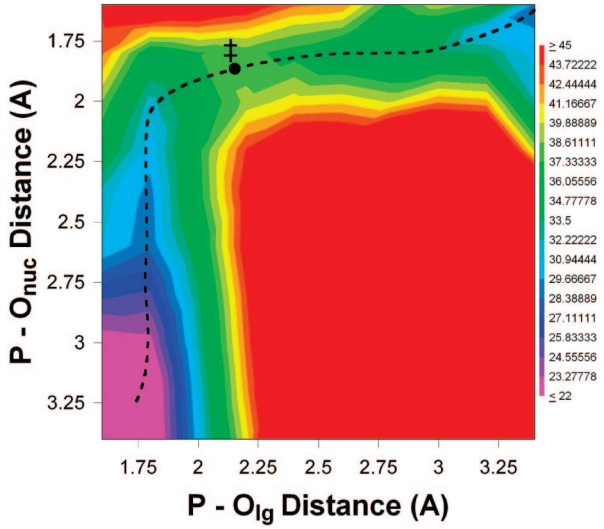


**FIGURE 5.** Free energy surface for hydroxide attack on dineopentyl phosphate. The concerted ($A_ND_N$) transition state is denoted by ‡.

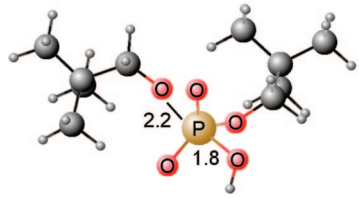


**FIGURE 6.** Transition state for hydroxide attack on dineopentyl phosphate.

**TABLE 1. Energy Decomposition of $\Delta G_{calc}$ for Hydroxide Attack on Monoanionic Dineopentyl Phosphate (Base-Catalyzed Reaction)[a]**

| | $\Delta E_{gas}$ | $\Delta\Delta G_{solv}$ | $\Delta E_{pol}$ | $-T\Delta S_{conf}$ | $\Delta G_{calc}$ | $\Delta G_{exp}$ |
|---|---|---|---|---|---|---|
| TS | 69.4 | −37.1 | 5.5 | 5.4 | 43.2 | 42.9 |

[a] TS denotes the concerted $A_ND_N$ transition state. $\Delta G_{exp}$ is derived from the rate constant measured at 250 °C.[49]

configurational entropies were calculated using the Molaris Software Package and the Enzymix forcefield.[64,65]

## Results and Discussion

**$HO^- + NpO_2PO_2^-$.** The free energy surface for hydroxide attack on dineopentyl phosphate is shown in Figure 5. For this system, the reaction is seen to proceed through a single concerted $A_ND_N$ pathway, via a transition state with P−O distances of 1.8 and 2.2 Å to the nucleophile and leaving group, respectively. This free energy surface is in good agreement with previous computational studies of hydroxide attack on phosphate diesters.[27] The structure for this transition state is shown in Figure 6, and the energy decomposition for $\Delta G_{calc}$ is shown in Table 1. The position of the transition state shown in Figure 5 suggests that there is more significant bond formation to the nucleophile in comparison to the amount of bond cleavage to the leaving group. In determining the character of the reaction pathway, it is helpful to not only take into account the isolated transition state geometry and bonding but also the overall reaction path, which is revealed by mapping the full free energy surface. In this case, close approach of the nucleophile to the phosphorus

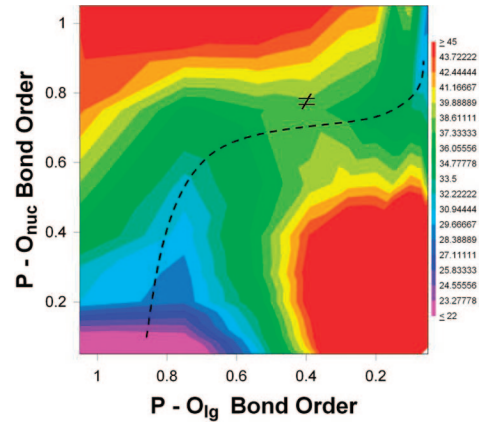


**FIGURE 7.** Free energy surface for water attack on dineopentyl phosphate depicted in terms of bond order. The concerted ($A_ND_N$) transition state is denoted by ‡.

center preceeds bond cleavage to the leaving group and the reaction trajectory passes close to the $A_N + D_N$ corner of the surface.

Figure 7 depicts the same free energy surface using bond order, $n$ (using the relationship $r = r_e - 0.6\ln(n)$), rather than bond distance as the coordinate system. Although this simplistic transformation should not be overinterpreted (for example, $r_e$ is different for the phosphate and phosphorane species; here, we have used $r_e$ for the phosphate starting and product states to normalize the bond order coordinates in the two dimensions), it does serve to highlight how the same data can lead to apparently different transition-state descriptions. From this plot, the transition state would appear to be nearly synchronous, with a slightly associative character (net increase in bond order from 1 to ~1.2). This is because the different parameters emphasize different changes—distance clearly provides geometrical data, but bond order is less readily interpreted, although traditionally this has been related to charge development by physical organic chemists. Experimentally, Brønsted parameters and Leffler indices[45] have been used to characterize reaction progress as if they report on bond order. More strictly, this analysis is linked to the fractional effective charge change that is reached in the transition state, relative to complete reaction. Again, in the trajectory pictured here, most of the bond order to the nucleophile is established early on the reaction pathway, followed by almost solely bond cleavage to the leaving group to reach the transition state.

The experimentally determined rate constant for this reaction at 250 °C is $(1.6 \pm 0.4) \times 10^{-5}$ $M^{-1}$ $s^{-1}$,[49,66] which from transition-state theory gives a value of 43 kcal/mol for $\Delta G_{exp}$. Our value of $\Delta G_{calc}$ (Table 1) is virtually identical to the experimental value, though it is likely that this exact agreement is coincidental.

**$H_2O + NpO_2PO_2^-$.** The free energy surface for water attack on dineopentyl phosphate is shown in Figure 8. Once again, the reaction proceeds through a single reaction pathway. However, in contrast to the previous system (Figure 5), the reaction now proceeds through a stepwise $A_N + D_N$ pathway. The geometries for the key stationary points of this pathway are shown in Figure 9, and the energy decomposition for $\Delta G_{calc}$ is shown in Table 2. In the first step of the reaction pathway, the reaction proceeds through a compact transition state (Fig-

(65) Chu, Z. T.; Villa, J.; Strajbl, M.; Schatz, C. N.; Shurki, A.; Warshel, A., *MOLARIS version beta9.05*; University of Southern California, 2004.

(66) Williams, N. H.; Wyman, P. Base Catalysed Phosphate Diester Hydrolysis. *Chem. Commun.* **2001**, 1268–1269.

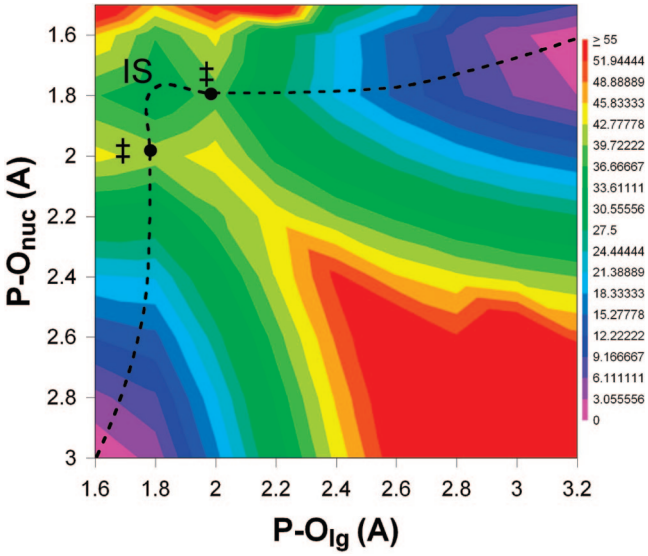


**FIGURE 8.** Free energy surface for water attack on dineopentyl phosphate. IS denotes an intermediate state, and ‡1 and ‡2 denote transition states for P−O$_{nuc}$ formation and P−O$_{lg}$ cleavage, respectively.

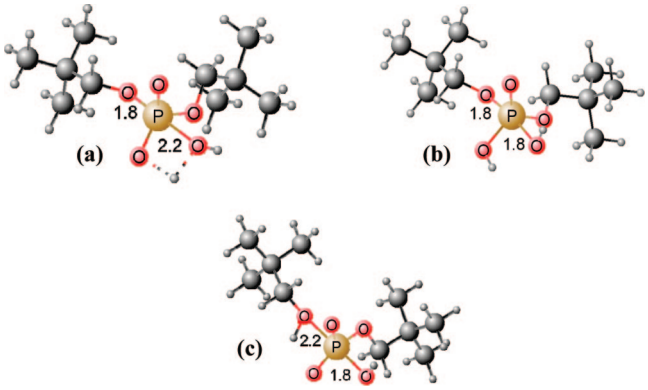


**FIGURE 9.** Key stationary points for water attack on the dineopentyl phosphate monoanion: (a) transition state for P−O formation to the nucleophile, (b) $A_N + D_N$ intermediate, and (c) transition state for P−O cleavage to the leaving group.

**TABLE 2. Energy Decomposition of $\Delta G_{calc}$ for Water Attack on Monoanionic Dineopentyl Phosphate (pH-Independent Reaction)[a]**

| | $\Delta E_{gas}$ | $\Delta\Delta G_{solv}$ | $\Delta E_{pol}$ | $-T\Delta S_{conf}$ | $\Delta G_{calc}$ | $\Delta G_{exp}$ |
|---|---|---|---|---|---|---|
| TS1 | 34.0 | 8.3 | −0.9 | 8.4 | 49.8 | ~46.0 |
| Int. | 20.5 | 15.8 | −2.7 | | 33.6 | |
| TS2 | 32.5 | 6.2 | −0.4 | | 38.3 | |

[a] This reaction proceeds through a stepwise ($A_N + D_N$) pathway. TS1 denotes the transition state for P−O$_{nuc}$ formation, IS the $A_N + D_N$ intermediate, and TS2 is the transition state for P−O$_{lg}$ formation. $\Delta G_{exp}$ is derived from the rate constant measured at 250 °C.[49,66]

ure 9a) with P−O distances of 2.2 and 1.8 Å to the nucleophile and leaving group, respectively. The barrier to this step is 50 kcal/mol which is within 4 kcal/mol of the experimental value of 46 kcal/mol (based on a rate constant of $(1 \pm 0.2) \times 10^{-6}$ s$^{-1}$ at 250 °C[49]). P−O bond formation occurs concomitantly with proton transfer from the attacking water molecule to a phosphate oxygen, resulting in the formation of a symmetrical $A_N + D_N$ intermediate with P−O distances of 1.8 Å to both the nucleophile and leaving group (Figure 9b). In the second step, the reaction proceeds through a transition state with P−O distances of 1.8 and 2.2 Å to the leaving group and nucleophile respectively (Figure 9c). In this step, the proton that was transferred to the phosphate oxygen in the first step is now transferred onto the departing leaving group, resulting in an alcohol and a monoanionic diester as products.

From Table 2 it can be seen that the first step (P−O formation to the nucleophile) is the rate-determining step. However, from Table 2 it can also be seen that TS1 (bond formation to the nucleophile) and TS2 (bond cleavage to the leaving group) are very similar in energy and, thus, that the barrier to the forward and reverse reactions from the intermediate (IS) are virtually identical. It should also be noted that even though we have not mapped out the energy surfaces to P−O distances that are long enough to reproduce a possible dissociative pathway, it can already be seen from Figure 8 that such a pathway, if it were to exist, would have a barrier that is at least 30 kcal/mol higher than the experimental pathway. Therefore, the dissociative pathway has been ruled out as a viable mechanism for the diester anion.

**Stepwise vs Concerted Proton Transfer.** There are two mechanistic possibilities for the case of water attack on the diester: hydrolysis can either proceed via water attack on a monoanion (eq 3) with concerted proton transfer or via a stepwise process involving hydroxide attack on a neutral diester by hydroxide ions that were formed in a pre-equilibrium step (eq 4).

$$H_2O + NpO_2PO_2^- \overset{k_1}{\rightleftharpoons} NpOH + NpOPO_3H^- \quad (3)$$

$$H_2O + NpO_2PO_2^- \overset{K}{\rightleftharpoons} OH^- + NpO_2PO_2H \overset{k_1}{\rightleftharpoons} NpOH + NpOPO_3H^- \quad (4)$$

Unfortunately, it is experimentally impossible to distinguish between eqs 3 and 4, as the overall rate constants have the same kinetic form. However, this issue can be investigated computationally, by carefully mapping the free energy surface for this system. The two possibilities (i.e., concerted proton transfer and stepwise proton transfer) are shown schematically in Figure 10.

In Figure 10, the concerted pathway is shown in purple and the stepwise pathway in green. $\Delta G_{PT}$ denotes the free energy for proton transfer from hydroxide to the substrate through a pre-equilibrium step, and $\Delta g^{\ddagger}_{SW}$ and $\Delta g^{\ddagger}_{CON}$ represent $\Delta g^{\ddagger}$ for the stepwise and concerted possibilities respectively. When setting up our system, we allowed the proton from the attacking nucleophile to freely follow the lowest energy path, and this resulted in the proton invariably starting on the nucleophilic oxygen then being transferred to a phosphate oxygen atom, resulting in the stepwise $A_N + D_N$ mechanisms shown in Figures 8 and 10. Mathematically, the activation barrier of the concerted pathway can represented as in eq 5:

$$\Delta g_{CON}^{\ddagger} = \Delta g^{\ddagger}\left((H_2O + NpO_2PO_2^-) \rightarrow (NpO_2PO_3H_2^-)\right) \quad (5)$$

The barrier of the stepwise pathway can be represented as shown in eq 6:[24]

$$\Delta g_{sw}^{\ddagger} = 2.3RT(pK_a(H_2O) - pK_a(NpO_2PO_2^-)) + \Delta g^{\ddagger}((HO^- + NpO_2PO_2H) \rightarrow (NpO_2PO_3H_2^-)) = \Delta G_{PT} + \Delta g_{OH}^{\ddagger} \quad (6)$$

The first term in eq 6 represents the energetics of the proton transfer step to the phosphate and the second term rep-

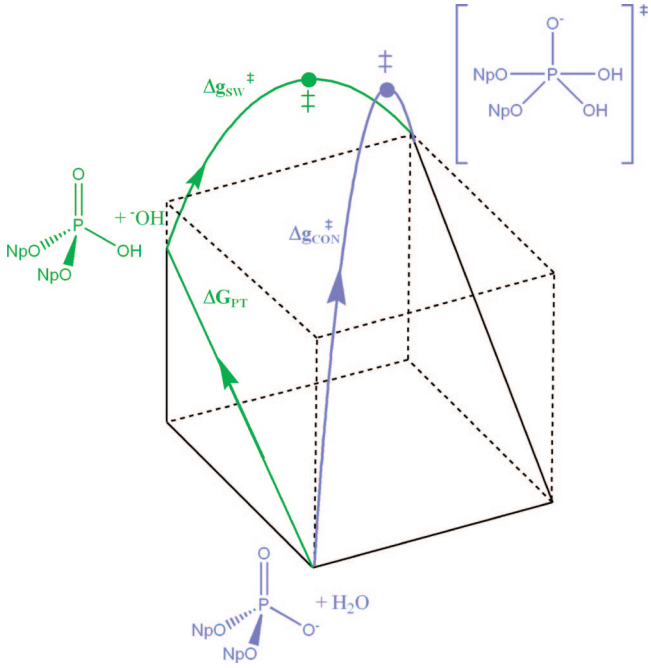


**FIGURE 10.** Schematic three-dimensional representation for stepwise vs concerted proton transfer. $\Delta G_{PT}$ denotes the free energy for proton transfer through a pre-equilibrium step, and $\Delta g^{\ddagger}_{SW}$ and $\Delta g^{\ddagger}_{CON}$ represent $\Delta g^{\ddagger}$ for the stepwise and concerted addition reactions, respectively. The concerted pathway is shown in purple and the stepwise pathway in green. ‡ denotes a transition state. The positions of the transition states on this figure are merely illustrative, and the actual transition states can occur at any point along the reaction path.

resents the barrier for hydroxide attack on the neutral phosphate. Thus, the energetics of the reactants for the second step of the stepwise process is determined by the p$K_a$ difference between the attacking water molecule and the phosphate (eq 7)

$$\Delta G_{PT} = 2.3RT\left(pK_a(H_2O) - pK_a\left(NpO_2PO_2^-\right)\right) \qquad (7)$$

which for this system would lead to a value of 17.8 kcal/mol for $\Delta G_{PT}$ at 250 °C (obtained from a p$K_a$ of 3.6 ± 0.3 for dineopentyl phosphate and a p$K_w$ of 11). Based on this, hydroxide attack on the neutral phosphate diester would have to have a significantly lower free energy than water attack on the phosphate monoanion (with concerted proton transfer) in order to be able to reproduce $\Delta G_{exp}$. We have examined the free energy surface for hydroxide attack on neutral phosphate and obtained a barrier of 12 kcal/mol for this reaction (see the Supporting Information). Therefore, for this system, hydroxide attack on the neutral phosphate appears to be sufficiently rapid, and the stepwise pathway is also a viable mechanism for this system.

**$H_2O$ + $NpO_2POH$.** The free energy surface for water attack on neutral dineopentyl phosphate is shown in Figure 11. Unlike the previous two systems, the reaction can now proceed through either a stepwise $A_N$ + $D_N$ pathway or a concerted $A_ND_N$ pathway. The stationary points for the two pathways are shown in Figures 12 and 13, and the energy breakdown for both pathways can be seen in Tables 3 and 4. In the stepwise $A_N$ + $D_N$ pathway, the reaction proceeds via a compact transition state with P−O distances of 1.7 and 2.0 Å to the leaving group and nucleophile, respectively (corresponding to P−$O_{nuc}$ formation, Figure 12a), to form a phosphorane intermediate (Figure 12b) in which a proton has been transferred from the attacking water

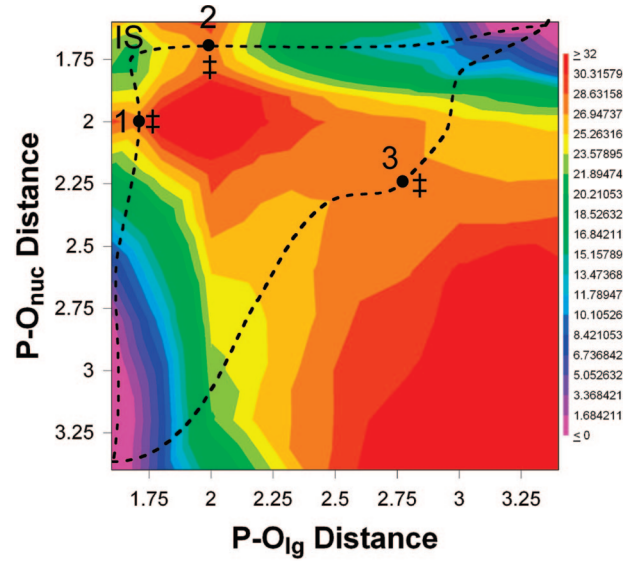


**FIGURE 11.** Free energy surface for water attack on dineopentyl phosphate. IS denotes an intermediate state, ‡1 and ‡2 denote $A_N$ + $D_N$ transition states for P−$O_{nuc}$ formation and P−$O_{lg}$ cleavage, respectively, and ‡3 denotes an $A_ND_N$ transition state.

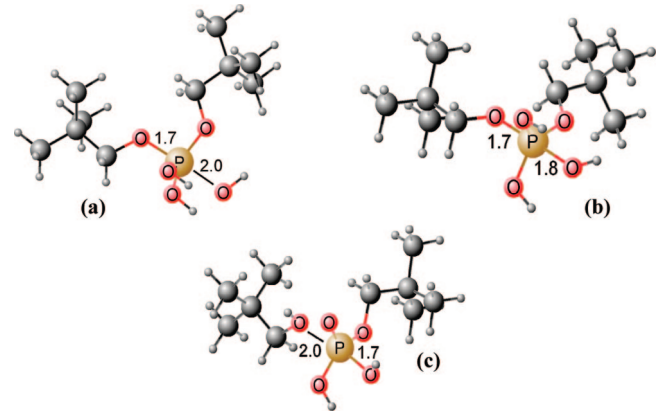


**FIGURE 12.** Key stationary points for water attack on neutral dineopentyl phosphate: (a) transition state for P−O formation to the nucleophile, (b) $A_N$ + $D_N$ intermediate, and (c) transition state for P−O cleavage to the leaving group.

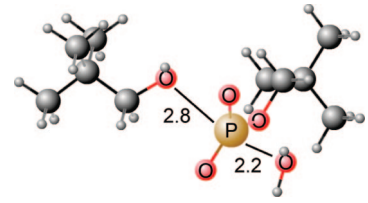


**FIGURE 13.** Concerted transition state for water attack on neutral dineopentyl phosphate.

molecule onto the phosphate. This proton is then transferred onto the leaving group and leaving group departure occurs via a second transition state with P−O distances of 2.0 and 1.7 Å to the leaving group and nucleophile, respectively (Figure 11c).

Here, all three species are slightly more compact than the corresponding species for water and hydroxide attack on the monoanion. In contrast, the $A_ND_N$ transition state is much more expanded with P−O distances of 2.8 and 2.2 Å to the leaving group and nucleophile, respectively (Figure 12). This pathway is rather dissociative in character, with bond cleavage advanced over bond formation; it should be noted that this transition state

**TABLE 3. Energy Decomposition of $\Delta G_{calc}$ for Water Attack on Neutral Dineopentyl Phosphate (Stepwise)[a] TS denotes the concerted $A_ND_N$ transition state. $\Delta G_{exp}$ is derived from the rate constant measured at 250 °C 49**

| | $\Delta E_{gas}$ | $\Delta\Delta G_{solv}$ | $\Delta E_{pol}$ | $-T\Delta S_{conf}$ | $\Delta G_{calc}$ | $\Delta G_{exp}$ |
|---|---|---|---|---|---|---|
| TS1 | 15.7 | −2.1 | 15.1 | 7.2 | 35.9 | 37.5 |
| int | 9.8 | −2.3 | 15.2 | | 22.7 | |
| TS2 | 19.9 | −1.5 | 10.1 | | 28.5 | |

[a] This reaction proceeds through a stepwise ($A_N + D_N$) pathway. TS1 denotes the transition state for P−$O_{nuc}$ formation, IS is the $A_N + D_N$ intermediate, and TS2 is the transition state for P−$O_{lg}$ formation. $\Delta G_{exp}$ is derived from the rate constant measured at 250 °C.[49,66]

**TABLE 4. Energy Decomposition of $\Delta G_{calc}$ for Water Attack on Neutral Dineopentyl Phosphate (Concerted)[a]**

| | $\Delta E_{gas}$ | $\Delta\Delta G_{solv}$ | $\Delta E_{pol}$ | $-T\Delta S_{conf}$ | $\Delta G_{calc}$ | $\Delta G_{exp}$ |
|---|---|---|---|---|---|---|
| TS | 22.8 | 6.2 | −0.8 | 8.2 | 36.4 | 37.5 |

[a] TS denotes the concerted $A_ND_N$ transition state. $\Delta G_{exp}$ is derived from the rate constant measured at 250 °C.[49]

lies on a shallow plateau of the energy surface. From Tables 3 and 4 it can be seen that both the $A_N + D_N$ and $A_ND_N$ pathways have almost identical values of $\Delta G^{\ddagger}_{calc}$ (35.9 and 36.4 kcal/mol respectively) and are thus indistinguishable. Also, these values lie within ∼2 kcal/mol of $\Delta G_{exp}$ (37.5 kcal/mol based on an experimental rate constant of 0.003 ± 0.001 $s^{-1}$ at 250 °C[31]).

**pH−Rate Profile.** We have examined three potential reaction mechanisms for hydrolysis of dineopentyl phosphate in this work: hydroxide attack on the dineopentyl monoanion and water attack on both the dineopentyl phosphate monoanion and the neutral species. In the first case, the reaction proceeds via a concerted ($A_ND_N$) mechanism, with a $\Delta G_{calc}$ of 43 kcal/mol. Hydroxide ion catalysis is only experimentally observed in very alkaline solution (pH > 13),[49] and we have reproduced the experimental barrier with high accuracy.

The full rate profile for the hydrolysis of dineopentyl phosphate can be easily constructed using the following general rate equation:

$$\nu = k_1[NpO_2PO_2H] + k_2[NpO_2PO_2^-] + k_3[HO^-][NpO_2PO_2^-] \quad (8)$$

The experimental first-order rate constant is defined by

$$\nu = k_{eff}[NpO_2PO_2(H)]_{total} \quad (9)$$

Therefore

$$k_{eff} = k_1([H^+]/([H^+] + K_a)) + (k_2 + k_3[OH^-])(K_a/([H^+] + K_a)) \quad (10)$$

where $K_a$ is the dissociation constant for the POH group in dineopentyl phosphate. In eqs 8 and 10, $k_1$ represents the rate constant for the reaction of the neutral diester (observed at low pH), $k_2$ the rate constant for the anion reacting with water, and $k_3$ the rate constant for the hydroxide-catalyzed reaction (observed at high pH). $k_1$, $k_2$, and $k_3$ were obtained from $\Delta G_{calc}$ for the water- and hydroxide-catalyzed reactions by use of transition-state theory and were found to be 0.016 $s^{-1}$, 2.1 × $10^{-8}$ $s^{-1}$, and 1.2 × $10^{-5}$ $M^{-1}$ $s^{-1}$ at 250 °C for the acid-catalyzed, pH-independent, and base-catalyzed reactions, respectively. Substituting these values back into eq 8 and plotting $k_{eff}$ vs pH yields the rate profile shown in Figure 14. Our theoretical rate profile shows a plateau up to pH 4 and a narrow pH-independent region around pH 10, with the reaction becoming hydroxide catalyzed after pH 12. As with the experimental rate profile presented in ref 49, the acid-catalyzed reaction at low pH dominates the reaction profile.

## Conclusions

Experimental studies on dineopentyl phosphate[49] have shown that the reaction is pH independent between pH ∼7 and ∼12, whereas at high pH, the reaction becomes hydroxide ion catalyzed.[49,66] In this work, we have compared the free energy surfaces for hydroxide and water attack on dineopentyl phosphate. We demonstrate that in the case of hydroxide attack, the reaction proceeds through a concerted ($A_ND_N$) associative pathway. However, in the case of water attack on the phosphate monoanion, there is a mechanistic switch toward a stepwise associative ($A_N + D_N$) pathway. Finally, in the case of water attack on neutral phosphate, the reaction can proceed through either a stepwise associative ($A_N + D_N$) or a concerted ($A_ND_N$) pathway. In all cases, we obtain values of $\Delta G_{calc}$ that are in good agreement with $\Delta G_{exp}$.

Conceptually, we can suggest a simple rationale for this change in mechanism. In the case of the base-catalyzed reaction, both incoming nucleophile and departing leaving group are anionic, with no proton transfer between nucleophile and subtrate. In this case, the reaction follows a simple $A_ND_N$ mechanism that is in good agreement with previous computational studies of phosphate diester hydrolysis.[67] However, in the case of water attack on either the monoanionic or neutral species, the situation becomes more complicated. Here, in all cases, we observe proton transfer from the attacking water molecule to the substrate. Furthermore, in the closely related transition state for the breakdown of the intermediate, the departing leaving group becomes protonated. Therefore, there is also a proton transfer to the leaving group. Considering the fact that in all our transition states the distance between $O_{nuc}$ and $O_{lg}$ is greater than ∼4 Å, it is highly unlikely that this proton transfer can occur directly from the nucleophile to the leaving group, which in the case of water attack on the monoanionic species is also the only proton source. For this system, this problem is circumvented by proceeding through a stepwise addition−elimination ($A_N + D_N$) mechanism in which the first step (bond formation between the phosphate and the incoming nucleophile) is accompanied by proton transfer to the phosphate to form a neutral phosphane intermediate, from which the leaving group can then extract a proton in the second step (leaving group departure). The central phosphoryl moiety is acting as a proton shuttle. This second step has similarities to the proposed rationale behind the reactivity of phosphate monoester monoanions, where protonation of the leaving group is the key driving force used to ratonalize the relatively high reactivity of these species. In that case, a high energy tautomer decomposes to a stable alcohol and high energy *m*-phosphate; here, a high energy phosphorane decomposes to a stable alcohol and stable phosphate ester.

Experimentally, it is very difficult to distinguish between concerted water attack on a monoanionic diester and hydroxide attack on neutral phosphate (i.e., via an unfavorable pre-

(67) Rosta, E.; Kamerlin, S. C. L.; Warshel, A. On the Interpretation of the Observed LFER in Phosphate Hydrolysis: A Thorough Computational Study of Phosphate Diester Hydrolysis in Solution. *Biochemistry* **2008**, *47*, 3725–3735.

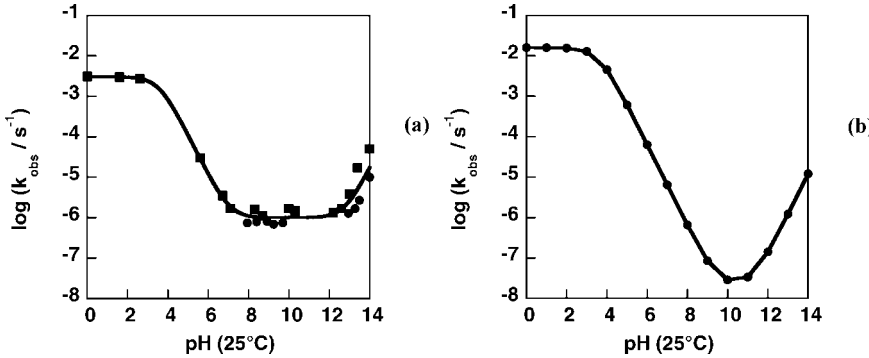


**FIGURE 14.** Experimental[49] (a) and calculated (b) rate profiles for the hydrolysis of dineopentyl phosphate, experimental buffer pH measured at 25 °C and reaction rates at 250 °C.

equilibrium proton transfer, as shown in Figure 2; solvent isotope effects might reveal whether a proton is in flight in the rate limiting transition state) to make the same intermediate. Our calculations suggest that the rate for hydroxide attack on the neutral species is fast enough, to compensate for the cost of $\Delta G_{PT}$. Thus, it is also plausible that this reaction can proceed through simple decomposition of the monoanionic phosphorane to form the alkoxide anion and neutral phosphate as the initial products.

In the case of the neutral species, the reaction can also proceed via a stepwise mechanism involving a fully protonated phosphorane intermediate that is reached through concomitant proton transfer to the phosphate as the P−O bond forms. Presumably owing to the greater electrophilicity of the neutral phosphate diester, this reaction is substantially faster than the corresponding reaction of the anion and dominates the pH rate profile up to pH 7.

However, the availability of an extra proton on the reactant phosphate now allows for a concerted $A_ND_N$ mechanism, in which the leaving group extracts this proton upon departure to yield inorganic phosphate and alcohol via a transition state that is dissociative in character. The central phosphoryl moiety is tending in structure toward a neutral phosphosphate ester, a species that has been implicated in the fragmentation of α-hydroiminophosphonates.[68] This again mirrors the behavior of phosphate monoester monoanions, and suggests a major role for intramolecular general acid catalysis using the phosphoryl OH. Both pathways have identical activation energies, suggesting that when there is a proton available for facile extraction by the departing leaving group, both stepwise and concerted pathways are equally viable.

The novelty of the present work is that we have examined the hydrolysis of dineopentyl phosphate over the entire pH range by means of mapping full free energy surfaces for the relevant reactions, and in doing so have demonstrated that at least in the case of the hydrolysis of dineopentyl phosphate, a stepwise pathway with the formation of a discrete phophorane intermediate is not only viable but, in the case of water attack on the monoanion, is the *only* pathway observed on the free energy surface. Furthermore, all these calculations suggest that intramolecular general acid catalysis by POH has a major role in the reactions of these diesters.

**Acknowledgment.** This work has been funded by NSF Grant No. MCB-0342276, and all computational work was supported by the University of Southern California High Performance Computing and Communication Centre (HPCC). Finally, we thank Robert Rucker for his assistance in the preparation of the manuscript.

**Supporting Information Available:** Free energy surface for hydroxide attack on neutral dineopentyl phosphate and coordinates of all key transition states and intermediates. This material is available free of charge via the Internet at http://pubs.acs.org.

JO801207Q

(68) Katzhenlder, J.; Schneider, H.; Ta-Shma, R.; Breuer, E. Fragmentation of Methyl Hydrogen Alpha-Hydroxyiminophosphonates - Kinetics, Mechanism and the Question of Metaphosphate Formation. *J. Chem. Soc., Perkin. Trans. 2* **2000**, 1961–1968.